DTIP of MEMS & MOEMS Stresa, Italy, 26-28 April 2006

HIGH CURRENT DENSITIES IN COPPER MICROCOILS: INFLUENCE OF SUBSTRATE ON FAILURE MODE

Johan MOULIN, Marion WOYTASIK, Jean-Paul GRANDCHAMP, Elisabeth DUFOUR-GERGAM, Alain BOSSEBOEUF

IEF, Université Paris XI, 91405 Orsay cedex, France

ABSTRACT

Copper planar microcoils were processed by U.V. lithography on SiO_2/Si and Kapton®. The coils were packaged on different supports in order to create varying thermal exchange conditions. The electric current was increased step by step until the electric connection breaks, the microcoils remaining free on a thermal point of view. The copper temperature was estimated from its resistivity. It allowed to show that the thermal exchange mode of the wire-bonded microcoils is conductive. The current density was calculated taking into account the deterioration of the coils by oxidation. Its maximum value is linearly decreasing with the thermal exchange ability of the support. The failure modes of the microcoils are related to track melting and oxidation, the current density remaining one order too weak to induce electromigration.

1. INTRODUCTION

Recent advances in microtechnology allow realization of planar microcoils. These components can be integrated as well as microinductive passive components or active devices like magnetic sensor or actuator in MEMS. As sensor, two major benefits are related to reduction of the coil dimension: the increasing of its spatial sensitivity and the feasibility of realizing matrix for magnetic field cartography. Applications are numerous in the domain of NDT (Non-destructive Testing) [1] or Magnetic Resonance Imaging (MRI) [2].

The shrinkage of the device used as actuator allows a local application of the magnetic field. In his aim, the microcoils can be part of micro-transformers [3,4] or electromagnetically actuated MOEMS [5,6]. Moreover, in order to optimize the magnetic field created, it is necessary to increase the current through the coil up to maximal value without damaging the device.

The present study consisted in applying harsh electrical conditions to the microcoils, in order to determine involved failure factors responsible for electrical connection break: electromigration, track or connection destruction by Joule effect, structural or physico-chemical modification, etc... Actually, the influence of high current densities is well known on conductive macroscopic devices and on microstrip or copper metallization layer which dimensions is in the order or 100-200 nm [7,8,9] to 1 µm [10]. On the other hand, its influence on 1-10 µm range electrical device has not been extensively studied, to our knowledge.

2. SAMPLES PREPARATION

The planar microcoils are fabricated using U.V. micromolding technology, which is of great interest since it allows a fast, low cost realization of thick metallic tracks (Fig. 1). During the process, one mask level only is necessary. The fabricated microcoils feature a central and an external electrical pad for bonding. They were processed on different substrates: flexible polymer (Kapton®) and silicate on silicon. It is to notice that the

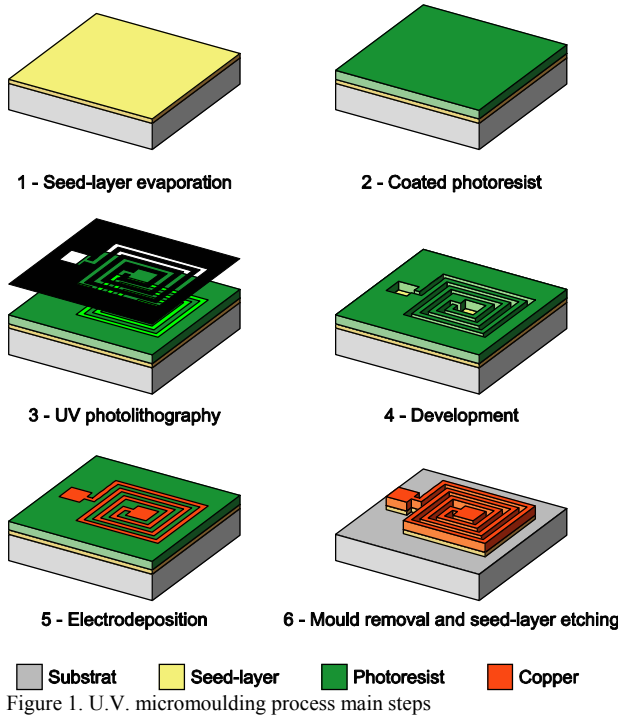

Figure 1. U.V. micromoulding process main steps

Sample	Substrate	Packaging	shape	# of turns	Track thickness (µm)	Track width (µm)	Inter-track (µm)
S1	Silicon	On-wafer	R	40	7	7	3
S2	Silicon	Epoxy card cyanoacrylic glu	S	40	6	10	4
S3	Silicon	TO 220 support cyanoacrylic glu	RS	40	6	6	4
S4	Silicon (same wafer than S3)	TO 220 support epoxy conducting resin	SO	40	6	6	4
S5	Silicon (same wafer than S3)	TO 220 support cyanoacrylic glu	SO	40	6	6	4
S6	Silicon (same wafer than S3)	TO 220 support mounted on a radiator	S	40	6	6	4
K1	Kapton (50µm)	Free Kapton	S	8	19	23	7

Table 1. Dimensions and packaging of the studied microcoils

process is quite similar for both substrate types. For more information, the reader can report to other paper from the authors [11].

Different shapes were defined: round (R), square (S), square with rounded angles (RS), squared round (SR) or square-octagonal (SO) coils. Nevertheless, the external dimension of the coils is 1 mm. The track width varies theoretically from 5 µm to 20 µm, but the optical lithography can introduce small variations. The track thickness is predetermined by the electrodeposition conditions (time and current density) but is limited by the photoresist thickness, i.e. 20 µm. The track thickness and width were precisely defined using optical interferometry and SEM observation respectively. The table 1 presents some geometrical characteristics of the studied microcoils and their packaging.

The packaging was designed in order to correspond to the more realistic configuration compared to future using of the microcoils. Concerning sample K1, the kapton film was glued to cover a hole made in an epoxy board, so the microcoil and its substrate are free and thermal exchange with support is minimized. Concerning samples S1 to S6 on silicon substrate, two measurement techniques were investigated, depending on the device package. On-chip microcoils were glued on different supports: epoxy board (S2) and MEMS package like TO220 support. Two different types of adhesive were tested: cyanoacrylic glue (S3 and S5) and epoxy conducting resin (S4). One of the supports was mounted on a radiator which surface is close to the one of a 2-inch wafer (S6). Finally, a microcoil was directly on-wafer characterized via tungsten carbide microprobes (S1).

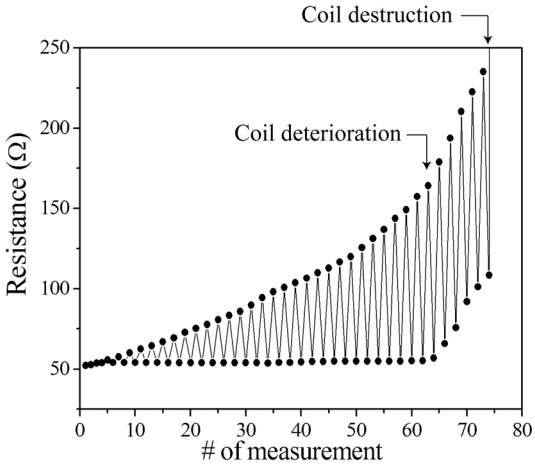

Figure 2. Typical measurement procedure of the resistance of a microcoil.

3. MEASUREMENT PROCEDURE

The experimental procedure consists in supplying the coil by DC current that is increased step by step up to the break of the electrical connection. At each step, the thermal equilibrium is waited for, then voltage and current are measured. The device is in-live inspected using an optical interferometer Zoomsurf 3D Fogale Nanotech.

The average temperature of the copper is estimated from its resistivity, starting from the hypothesis that the resistivity is linearly dependent with the temperature variation:

$$\rho_T = \rho_{T_{amb}} \left(1 + \alpha_{th} \left(T - T_{amb}\right)\right)$$

with α_{th} the temperature coefficient, that is equal to 4.3 10^{-3} K^{-1} for the copper and $\rho_{T_{amb}}$ the resistivity of the electrolytic copper at ambient temperature. Its value is equal to that of the massive one, i.e. ρ_{Cu} = 1.7 10^{-8} Ω m, as previous works confirmed [1].

The electrical resistance depends itself on the geometrical parameters and the resistivity of the copper track:

$$R_T = \rho_T \frac{\ell}{S}$$

with ℓ the length of the copper track and S its cross-section. In order to take into account eventual changing in the coil cross-section due to the heating, the supplied current is decreased to a weak value after each measurement and the initial resistance of the coil (named 'cold' resistance below) is checked.

sample	$R_{th\ eq.}$ (K W^{-1})	T_{det} (°C)
S1	45	192
S2	350	348
S3	200	297
S4	180	269
S5	190	294
S6	37	166
K1	1400	347

Table 2. Equivalent thermal resistance of the devices and temperature corresponding to the beginning of the coil deterioration.

The figure 2 presents each measurement step of the sample S3. Using the resistance value at cold temperature, the cross-section of the coil is estimated. This latter is then injected in the next step for calculation of the electric resistivity. Then its relative increasing leads to the value of the temperature increasing.
After measurements, the coil microstructure was observed using a Hitachi 3600 scanning electron microscope coupled with an EDS detector in order to check the microstructure and the composition of the track.

4. RESULTS

The electrical behavior of the microcoils during measurement process is characterized by three steps. First, while the current through the device increases, the copper is heated by Joule effect. The electric power injected in the material is dissipated by thermal exchange with the air or the support. The second step is characterized by the deterioration of the coil due to copper oxidization or track melting. This phenomenon is particularly lowering, because the track shrinking contributes to a current density increasing then to a temperature elevation. This behavior leads to the loose of the electric contact, when track is totally oxidized or cut.

4.1. Non-deterioration domain

4.1.1. Thermal behavior

The drawing of the copper temperature as a function of the electric power injected in the microcoils brings to the fore which of the thermal propagation mode is predominant (see Fig. 3). This drawing is quite linear during the first step for almost all the studied microcoils. This corresponds to thermal conduction and allows the determination of an equivalent thermal resistance:

$$P_{dissipated} = P_{cond.} = \frac{\Delta T}{R_{th}}$$

The table 2 presents the R_{th} values corresponding of both microcoil and support. There is a correlation between their values and the thermal resistivity of the support material. This is confirmed by the higher R_{th} values for coil on free Kapton than on transistor-type support, that are themselves higher than that of coil on transistor-type support mounted on radiator.
The similar results for the samples S3, S4 and S5 show that neither glue nor the form of the coils seems to have a obvious influence on the thermal behavior of the device.
The on-chip microcoil S1 presents a non-linear behavior because both thermal conduction and convection exchange mode are responsible for the thermal dissipation. This power can be simply modelized by:

$$P_{dissipated} = P_{cond.} + P_{conv.} = \frac{\Delta T}{R_{th}} + hS\left(T_{copper} - T_{amb}\right)^{0,25}$$

with h a factor depending on the material (h = 5 W m^{-2} K^{-1} is a classical value) and S the exchange area with the ambient air.
The fit of the injected power gives an equivalent thermal resistance of 45 K W^{-1}, which is comparable to the one of the microcoil mounted on a radiator (S6). The equivalent exchange surface with the air is several order higher compared to the microcoil area. This confirms that an important part of the wafer is heated and is involved in the thermal exchange.

4.1.2. Electrical behavior

The electric current in the microcoils is in the 10-100 mA range. The corresponding current density J in the microcoil track has been calculated and is in the order of

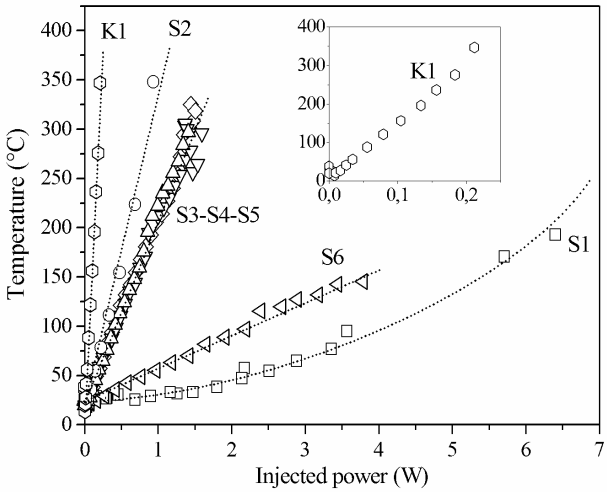

Figure 3. Copper temperature as a function of the injected electric power in the non-deterioration domain.

0.1 MA cm^{-2}. It is to notice that a scale effect is kept, as maximum current density in mm-sized and 0.1 µm-sized copper wires is in the order of 0.001 MA cm^{-2} and 10 MA cm^{-2} respectively. That can be express as:

$$J_{max} \approx \frac{1}{D^{(\mu m)}} \text{MA cm}^{-2}$$

with D the dimension of the conductive material.

The fig. 4 shows that the current density increases with the copper temperature, but saturates to a limit value. This limit is reached while the deterioration of the coil begins, what is represented by the filled forms and dot line in the figure. So the current density is related to the thermal exchange capacity of the support, Kapton being the worst of them.

4.2. Coil deterioration

4.2.1. Non-deterioration limit

The deterioration limit can be correlated to current density and copper temperature (see table 2 and 3). It can approximately express as following:

$$J_{det}^{(\text{MA cm}^{-2})} \simeq 1.4 - 3.6\,10^{-3} T_{det}^{(°C)}$$

This expression is particularly useful for the dimensioning of the microcoils that can be involved in magnetically actuated MEMS or in inductive components.

sample	J_{det} (MA cm^{-2})	P_{det} (W)
S1	0.58	6.5
S2	0.17	0.95
S3	0.37	1.4
S4	0.38	1.4
S5	0.36	1.3
S6	0.78	3.8
K1	0.062	0.21

Table 3. Current density and injected power at the beginning of the coil deterioration.

4.2.2. Deterioration factors

The measurement procedure consists in the verification of the microcoil resistance at low current after each measurement. This checking shows that physical deterioration of most of the coils begins while the temperature of the copper reaches a value depending on the thermal properties of the device. At this stage, the cold resistance of the coils is higher than the initial one. This irreversible changing is a consequence of a reduction of the track section. It is supposed that oxidation is responsible for this phenomenon. Actually, as an example, the resistance of the coil K1 just before connection break is equivalent to that of a track with a 5 µm oxide layer at the surface. In addition, EDS analysis of the same sample gave an oxygen ratio decreasing from 40 at.% at 5 kV acceleration voltage to 32 at.% at 30 kV. This corresponds to a thick copper oxide layer. Actually, Monte-Carlo simulation showed that even at 5 kV, the electrons penetration depth in copper oxide CuO is larger than 5 µm.

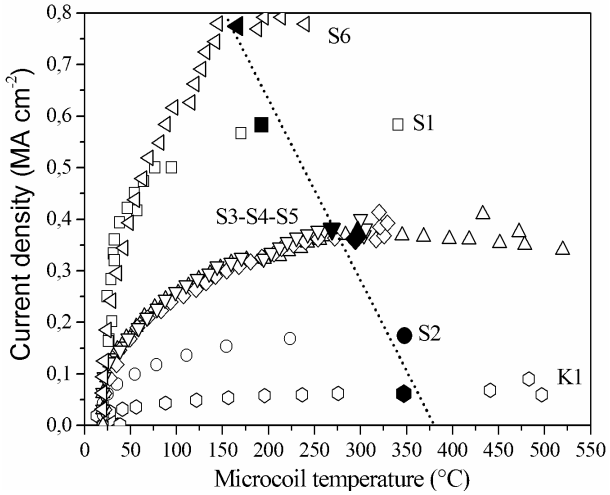

Figure 4. Current density in the microcoils as a function of their temperature. Filled forms (and fitting dot line) represent the limit of the non-deterioration domain.

As an exemple, the fig 5 presents a part of the sample S3 at different stages of the measurement procedure until the electrical connection is broken. The track morphology has been build using interferograms. It remains quite flat below 300°C. Then, once the deterioration of the coil begins, the surface of the copper becomes irregular. It is

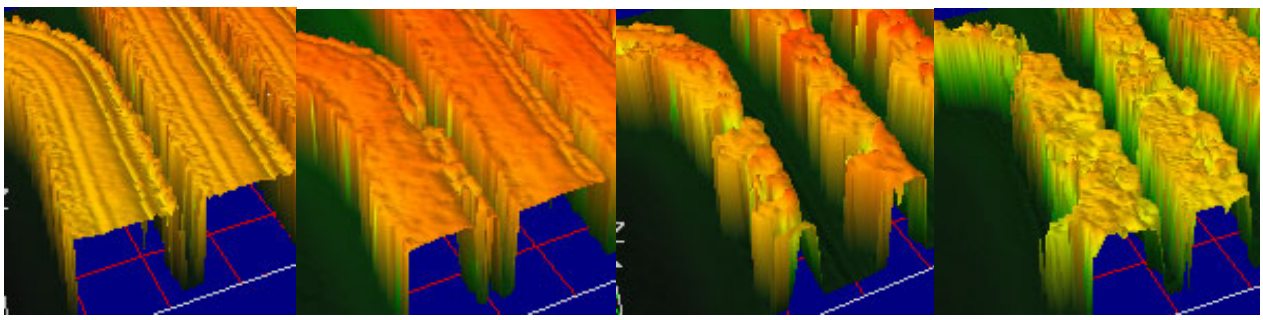

Fig.5. 3D Reconstruction of the track morphology using optical interferometry at different step of the measurement procedure (beginning, middle power, non-deterioration limit and non-destruction limit).

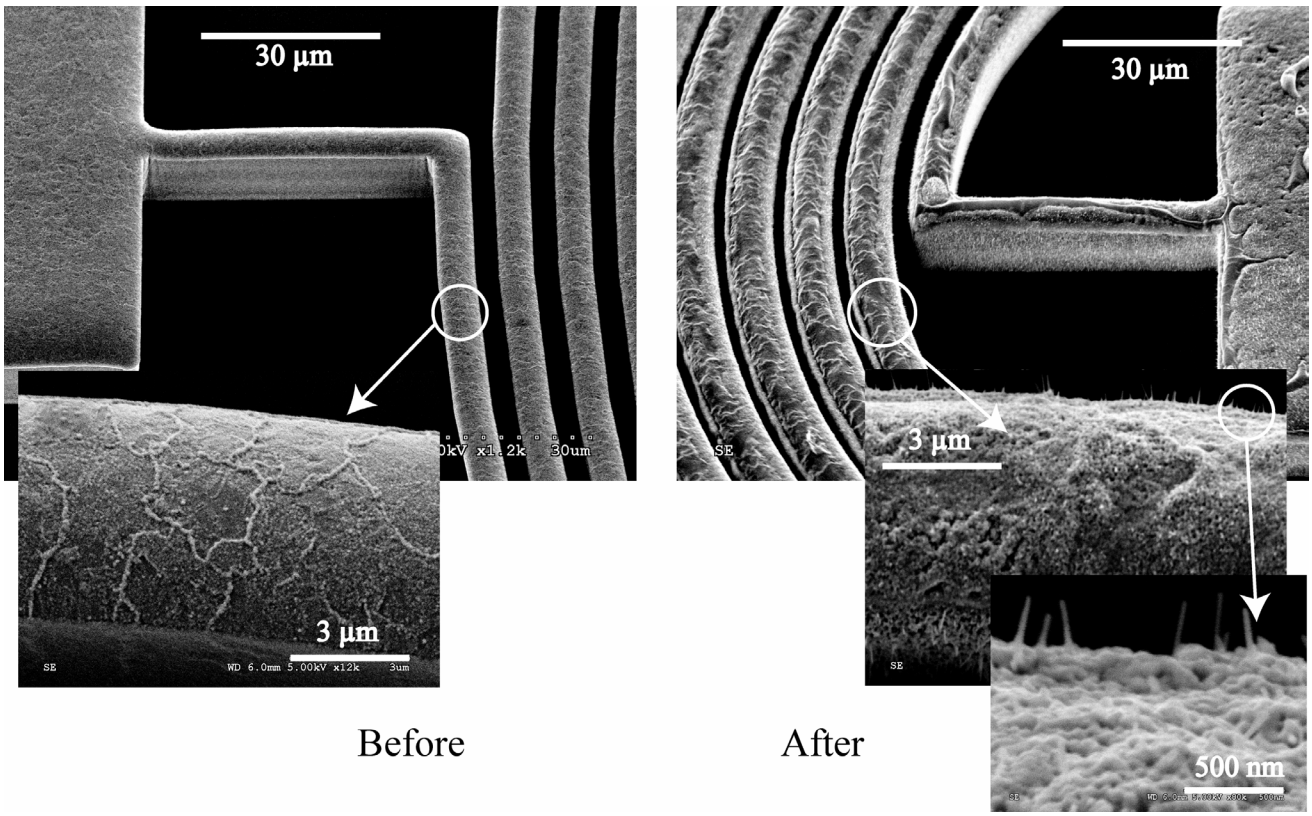

Figure 6. SEM observation of the sample S1 before and after the measurement procedure. The surface copper becomes irregular and is covered with nano-needles.

to notice that oxidized copper is optically dark and appears as melted copper, especially near the track border. As optical characterization by interferometry is limited to reflecting surfaces, the technique doesn't allow complete reconstruction of the 3D structure of the tracks.

SEM observation completed the study and showed both macro- and microstructure of the deteriorated coils. Pictures of the sample S1 after and before the complete measurement procedure are presented in the fig 6. The copper visibly melted at the top of the track that becomes rounded compare to its sharp and flat surface before the study.

In addition, all the studied microcoils present after the measurement procedure a surface covered with nano-needles (see fig 6). The size of these needles is around 200 nm long and 50 nm thickness. It is not possible for the moment to be sure of the composition of these needles, but it is supposed to be copper oxide.

4.3. Failure modes

Beyond the non-deterioration point, the heating of the microcoil is irreversible. While supplied voltage is increased again, the electric power follows it proportionally, because the current is saturated. The thermal exchange with the environment is from this point not enough to evacuate copper heat. So the temperature increases up to the electrical break. This maximal value corresponds to the last point of each curve of the fig. 4.

It is to notice that the observed failure modes depend from the substrate type. The samples processed on silicon and wired (S2, S3, S4, S5 and S6) failed because of both track oxidation and melting. This has already been discussed previously.

It is suppose that the electrical connection break was due to the same factors for microcoil on Kapton. Actually, EDS measurement showed that the copper was oxidized and it was not found any visible track cutting or bonded wire removing. In addition, the reduced thermal exchange ability of the substrate forced the copper to completely melt (see fig 7). The high temperatures leaded to the sublimation of the Kapton that released the track.

Finally, it was not possible to define precisely the failure mode of the sample S1 (on-wafer micro-coil). Actually, the high temperatures in the copper induced stress in the wafer, that bulged. Finally it broke the tungsten carbide microprobes. It was possible to estimate this bulging at around 50 µm using the optical interferometer focus. The last measurement point corresponds in fact to the microprobes break, not to the destruction of the coil.

5. CONCLUSION

The resistance measurement of the microcoils processed on silicon and Kapton mounted on different supports allows an exploration of the devices thermal and electrical limits.
The study gives some useful elements for the dimensioning of magnetically actuated devices or inductive components involving microcoils.
Despite the advantage of flexibility, polyimide substrate as Kapton presents a weak thermal conductivity that limits the thermal dissipation between coil and environment. Nevertheless, the current density reached in microcoils on Kapton remains 100 times higher than that in macroscopic wires, without damage.
Concerning failure modes, it was shown that mechanical distortion of the substrate can be the limitative factor for on-wafer microcoils. In case of sawed, glued on support and bonded on-chip coils, oxidation and melting of the copper track is responsible for the electrical connection break.

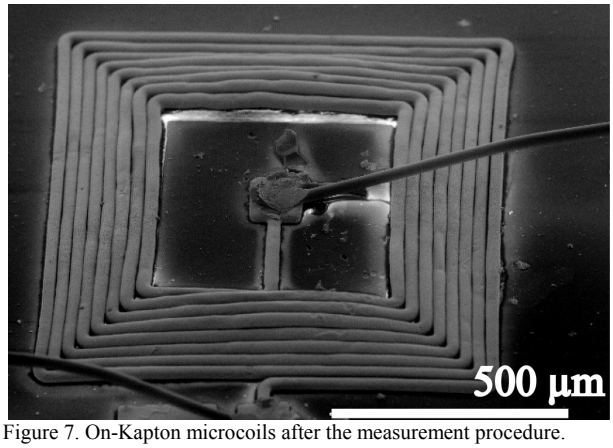

Figure 7. On-Kapton microcoils after the measurement procedure.

ACKNOLEDGEMENTS

This work was supported by the European network of excellence Patent DfMNN (Design for Micro & Nano Manufacture).

REFERENCES

[1] A.-L. Coutrot et al.*;* "Electromagnetic micro-device realized by electrochemical way", *Sensors and Actuators A*, vol. 91 (1-2), pp. 80-84, 2001

[2] A.-L. Coutrot et al. "Copper micromolding process for NMR microinductors realization*", Sensors and Actuators A*, vol. 99 (1-2), pp. 49-54, 2002

[3] E Martincic, et al., "Magnetic micro-transformers realizedwith a flip-chip process", Journal of. Micromechanics and Microengineering . vol.14, pp 5558, 2004

[4] R. M. H. Atta, "Multi-layer double coil micro-fabricated transformer", *Sensors and Actuators A: Physical*, vol. 112 (1), pp 61-65, 2004

[5] M.R.J. Gibbs, "Applications of magmems", *Journal of Magnetism and Magnetic Materials*, vol. 290-291 (2), pp 1298-1303, 2005

[6] O. Cugat, J. delamare and G. Reyne, "Magnetic Micro-Actuators and Systems (MAGMAS)", *IEEE Transactions on Magnetics*, vol. 36 n°5, pp 3607-3612, nov. 2003

[7] K.N. Tu, "Recent advances on electromigration in very-large-scale-integration of interconnects", *Journal of Applied Physics*, vol. 94 n°9, pp 5451-5473, nov. 2003

[8] H. Wendrock et al., "Correlation of electromigration defects in small damascene Cu interconnects with their microstructure", *Microelectronic Engineering*, vol. 82, pp 660-664, 2005

[9] G. Schindler et al., "Reliability studies of narrow Cu lines", *Microelectronic Engineering*, vol. 82, pp 645-649, 2005

[10] O. Kraft and E. Arzt, "Electromigration mechanism in conductor lines: void shape changes and slit-like failure", Acta Metallurgica, Vol. 45 n°4, pp 1599-1611, 1997

[11] M. Woytasic et al., "Fabrication of planar and three-dimenional microcoils on flexible substrates", *Microsystem Technologies*, to be published